The Canadian Mineralogist
Vol. 58, pp. 403-410 (2020)
DOI: 10.3749/canmin.2000010

ADANITE, A NEW LEAD-TELLURITE-SULFATE MINERAL FROM THE NORTH STAR MINE, TINTIC, UTAH, AND TOMBSTONE, ARIZONA, USA

ANTHONY R. KAMPF[§]

Mineral Sciences Department, Natural History Museum of Los Angeles County,
900 Exposition Boulevard, Los Angeles, California 90007, USA

ROBERT M. HOUSLEY AND GEORGE R. ROSSMAN

Division of Geological and Planetary Sciences, California Institute of Technology, Pasadena, California 91125, USA

HEXIONG YANG AND ROBERT T. DOWNS

Department of Geosciences, University of Arizona, 1040 4th Street, Tucson, Arizona 85721-0077, USA

ABSTRACT

Adanite, $Pb_2(Te^{4+}O_3)(SO_4)$, is a new oxidation-zone mineral from the North Star mine, Tintic district, Juab County, Utah, and from Tombstone, Cochise County, Arizona, USA. The characterization of the species is based principally on North-Star holotype material. Crystals are beige wedge-shaped blades, up to about 1 mm in length, in cockscomb intergrowths. The mineral is transparent with adamantine luster, white streak, Mohs hardness 2½, brittle tenacity, conchoidal fracture, and no cleavage. The calculated density is 6.385 g/cm^3. Adanite is biaxial (–), with $\alpha = 1.90(1)$, $\beta = 2.04$(calc), $\gamma = 2.08$(calc), $2V$(meas) $= 54(1)°$. The Raman spectrum is consistent with the presence of tellurite and sulfate groups and the absence of OH and H_2O. Electron-microprobe analyses gave the empirical formula $Pb_{1.89}Sb^{3+}{}_{0.02}Te^{4+}{}_{0.98}S^{6+}{}_{1.04}Cl_{0.02}O_{6.98}$. The mineral is monoclinic, space group $P2_1/n$, with $a = 7.3830(3)$, $b = 10.7545(5)$, $c = 9.3517(7)$ Å, $\beta = 111.500(8)°$, $V = 690.86(7)$ Å^3, and $Z = 4$. The four strongest X-ray powder diffraction lines are [d_{obs} Å(I)(hkl)]: 6.744(47)($\bar{1}01$), 3.454(80)($\bar{2}11, \bar{1}22, 200$), 3.301(100)($\bar{2}02, 031, 210$), and 3.048(73)($112, \bar{2}21, \bar{1}13$). The structure ($R_1 = 0.022$ for 1906 $I > 2\sigma I$ reflections) contains $Te^{4+}O_3$ pyramids that are joined by short (strong) Pb–O bonds to form sheets. Interlayer SO_4 groups link the sheets *via* long Pb–O and Te–O bonds.

Keywords: Adanite, new mineral, tellurite, sulfate, crystal structure, Raman spectroscopy, North Star mine, Tintic, Utah, Tombstone, Arizona, USA.

INTRODUCTION

Most cations in ionically bonded structures are approximately centered in their coordination environments. In contrast, cations with lone electron pairs have off-center coordinations when the lone pairs are stereoactive, that is, when they are oriented on one side of the cation rather than being symmetrically distributed. These off-center coordinations have short (strong) cation–anion bonds on the side opposite the lone pairs and much longer bonds on the same side as the lone pairs. Structures in which all or most of the cations have stereoactive lone pairs generally exhibit connectivities dominated by these short cation–anion bonds.

Adanite, the new mineral described herein, contains two different cations, Te^{4+} and Pb^{2+}, both with stereoactive lone pairs. This combination of cations is also found in the mineral northstarite, $Pb_6(Te^{4+}O_3)_5(S_2O_3)$ (Kampf *et al*. 2020), which occurs in direct association with adanite. In both cases, Te^{4+} and three strongly bonded O atoms form pyramidal tellurite groups, $(Te^{4+}O_3)^{2-}$. Interestingly, northstarite also contains a thiosulfate group, $(S_2O_3)^{2-}$, whereas adanite contains a sulfate group, $(SO_4)^{2-}$. Northstarite

---

[§] *Corresponding author e-mail address*: akampf@nhm.org and adanite are the only minerals currently known to contain only Pb^{2+}, Te^{4+}, S^{6+}, and O^{2-}; although recent studies of fairbankite, $Pb(Te^{4+}O_3)$, show it to contain $(SO_4)^{2-}$ sharing a $(Te^{4+}O_3)^{2-}$ site (Missen *et al*. 2020). Perhaps not surprisingly, the structures of both northstarite and adanite are unique and add to our knowledge of structures dominated by lone-pair cations.

The mineral is named adanite (\'eɪ dæn aɪt\) in honor of American systematic mineral collector/micromounter Charles (Chuck) Adan (b. 1961) of Salt Lake City, Utah, USA. Mr. Adan, a former President of the "Mineral Collectors of Utah" club in Salt Lake City, has self-collected most of his rare mineral collection. He is the discoverer of pararaisaite (Kampf *et al*. 2018a), northstarite (Kampf *et al*. 2020), and adanite (described herein), and he provided the holotype specimens for all three species. Mr. Adan has provided other specimens for scientific study, as well. Charles Adan has given permission for the mineral to be named in his honor. We recognized that the proposed name is very similar in spelling to adamite; however, it has a very different pronunciation (with a long 'A' at the beginning) and seemed much preferable to the double-name alternatives "charlesadanite" and "chuckadanite".

The new mineral and name have been approved by the Commission on New Minerals, Nomenclature and Classification of the International Mineralogical Association (IMA2019-088). The holotype specimen is housed in the collections of the Mineral Sciences Department, Natural History Museum of Los Angeles County, 900 Exposition Boulevard, Los Angeles, California 90007, USA, catalogue number 67505. Note that this specimen was originally attached to the holotype specimen of northstarite, catalogue number 67291. The cotype specimen from Tombstone is deposited with the RRUFF Project (University of Arizona), deposition number R190033.

OCCURRENCE

The mineral was first discovered at the North Star mine, Mammoth, Tintic district, Juab County, Utah, USA (39°55.23′ –112°6.45′). The North Star mine exploited a polymetallic (Au-Ag-Cu-Pb) vein deposit emplaced in contact-metamorphosed dolomite and was the largest producer of gold in the Tintic district. The North Star mine was discovered in 1885, closed in 1900, and reported to be inaccessible as of 1911. The principal ore minerals were galena, cerussite, and enargite and the prominent gangue minerals were quartz and barite (Lindgren & Loughlin 1919). A wide variety of oxidation-zone minerals has been collected from the mine dumps by collectors.

At the North Star mine, the mineral is known from only one small specimen. It occurs in a vug in massive quartz-baryte-enargite-pyrite. Other secondary minerals found in association with adanite are anglesite, azurite, chrysocolla, fluorapatite, northstarite, plumbogummite, tellurite, zincospiroffite, and an unidentified poorly crystalline Cu-tellurite. The mineral was collected and provided for study by Charles Adan of Salt Lake City, Utah, USA.

Adanite has also been confirmed in a specimen from Tombstone, Cochise County, Arizona, USA. This specimen was originally labelled only as frohbergite. On this specimen, adanite occurs as white massive crystalline aggregates on small euhedral jarosite crystals that coat the surface of the matrix. Frohbergite is found in veins in the matrix. Rodalquilarite is also found on the specimen. Because the only mine in the Tombstone district from which frohbergite has been previously reported is the Joe mine (or Joe shaft), this is most likely the origin of this specimen.

Adanite is an oxidation-zone mineral at both localities. All data reported herein are for adanite from the North Star mine; however, compositional and structural data obtained for the Tombstone material are completely consistent with data for North Star adanite. Tombstone should be considered the cotype locality for adanite.

PHYSICAL AND OPTICAL PROPERTIES

Adanite crystals from the North Star mine are beige, while those from Tombstone are colorless. They are wedge-shaped blades, elongate on [100] and flattened on {010}, up to about 1 mm in length (Fig. 1). Because of the complexity of the crystals and the curvature of some faces, the only form that could be reliably determined is {010}. Other forms that are likely, based on the general shape of the crystals and shape measurements obtained during the single-crystal XRD study, include {001}, $\{10\bar{1}\}$, $\{10\bar{2}\}$, {021} and $\{11\bar{1}\}$. No twinning was observed. The streak is white, the luster is adamantine, and crystals are transparent to translucent. The mineral does not fluoresce under long- and short-wave ultraviolet light. The Mohs hardness is about 2½ based on scratch tests. The tenacity is brittle, no cleavage was observed, and the fracture is conchoidal. The density could not be measured because it is greater than available density liquids and there is insufficient material for direct measurement. The calculated density is 6.385 g/cm^3 for the empirical formula and 6.595 g/cm^3 for the ideal formula, in both cases

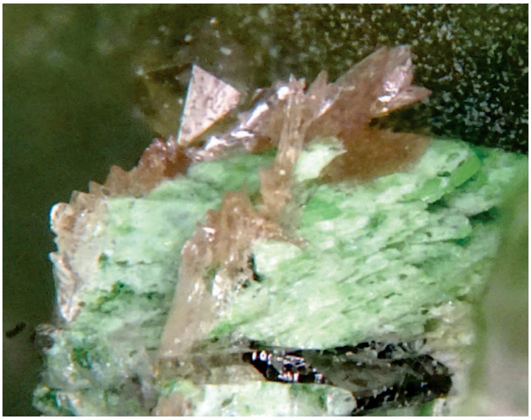

FIG. 1. Beige adanite crystals from the North Star mine on a poorly crystalline green Cu-tellurite phase. The field of view is 1.65 mm across.

on the basis of the unit-cell parameters refined from single-crystal XRD data. At room temperature, the mineral is very slowly soluble in dilute HCl, but rapidly soluble in concentrated HCl.

Optically, the mineral is biaxial (–), with α = 1.90(1), measured in white light. Both β and γ are greater than 2.0; because index liquids with $n > 2$ were unavailable, β and γ could not be measured. The γ–α birefringence (0.18) was measured using a Berek compensator and 2*V* was measured [54(1)°] using extinction data analyzed with EXCALIBRW (Gunter *et al*. 2004). This allowed the calculation of β and γ, 2.04 and 2.08, respectively.

TABLE 1. ANALYTICAL DATA (wt.%) FOR ADANITE

Constituent	Mean	Range	SD	Standard
PbO	61.61	61.03–62.14	0.58	Galena
Sb_2O_3	0.33	0.12–0.44	0.13	Sb metal
TeO_2	22.84	22.48–23.24	0.22	Te metal
SO_3	12.15	12.03–12.31	0.08	Anhydrite
Cl	0.09	0.05–0.11	0.02	Sodalite
O=Cl	–0.02			
Total	97.00			

RAMAN SPECTROSCOPY

Tellurate and tellurite minerals generally have strong diagnostic Raman spectra and the Caltech Mineral Spectroscopy Laboratory has compiled a searchable library containing many of these spectra. In the fall of 2018, Chuck Adan sent several minerals from the North Star mine for evaluation. Raman spectra of these were recorded using a Renishaw M1000 micro-Raman spectrometer system with a 2400 gr/mm diffraction grating. Light from a 514.5 nm solid-state laser was focused through a Leica microscope onto the samples. Adanite and the associated new mineral northstarite were flagged as a potentially new tellurites during this Raman survey. Furthermore, it was noted that the spectra for these two phases were essentially featureless between 4000 and 1200 cm^{-1}, consistent with them being anhydrous.

After a polished section of adanite was prepared, but before it was carbon coated, additional Raman spectra were obtained at Caltech, this time using a

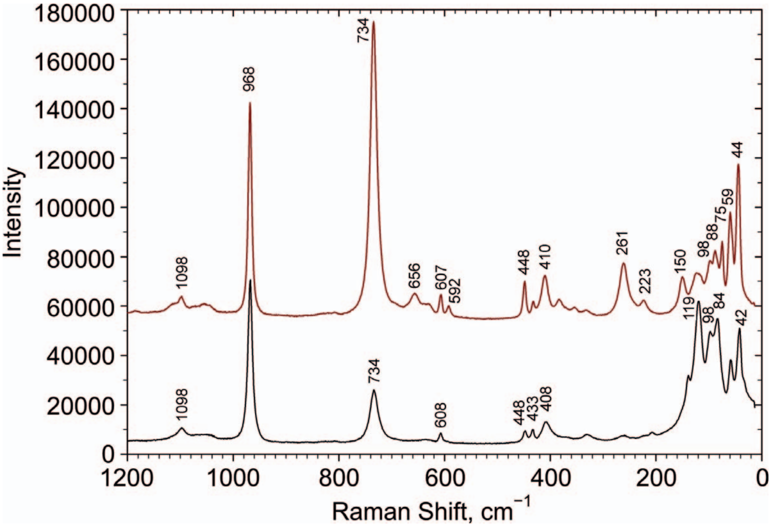

FIG. 2. The Raman spectra of two differently oriented adanite crystals recorded with a 514.5 nm laser.

TABLE 2. POWDER DATA (*d* IN Å) FOR ADANITE

I_{obs}	I_{calc}	d_{obs}	d_{calc}	*hkl*
47	34	6.744	6.7211	$\bar{1}01$
	5		5.3773	020
31	12	4.335	4.3505	002
17	12	4.223	4.2520	111
	7		4.2342	120
	4		4.0330	012
	7		3.5082	121
80	4	3.454	3.4901	$\bar{2}11$
	34		3.4486	122
	16		3.4346	200
100	12	3.301	3.3605	$\bar{2}02$
	57		3.3145	031
	32		3.2718	210
	9		3.1630	$\bar{1}31$
42	28	3.114	3.1117	$\bar{1}03$
73	23	3.048	3.0542	112
	32		3.0424	$\bar{2}21$
	14		2.9891	$\bar{1}13$
	6		2.8946	220
	4		2.8498	$\bar{2}22$
41	29	2.803	2.8026	$\bar{1}32$
44	4	2.745	2.7666	032
	8		2.7613	211
	24		2.7406	122
	4		2.6932	$\bar{1}23$
	4		2.6886	040
	5		2.6850	$\bar{2}13$
20	15	2.569	2.5712	$\bar{2}31$
	4		2.5527	023
9	5	2.482	2.4801	230
	3		2.4644	$\bar{2}23$
7	5	2.377	2.3851	$\bar{3}11$
8	6	2.317	2.3218	113
	3		2.2814	$\bar{1}14$
	3		2.2628	212
33	4	2.246	2.2548	033
	18		2.2404	$\bar{3}03$
39	8	2.181	2.1933	$\bar{3}13$
	14		2.1747	123
	6		2.1729	$\bar{2}41$
7	8	2.140	2.1415	$\bar{1}24$

TABLE 2. CONTINUED.

I_{obs}	I_{calc}	d_{obs}	d_{calc}	*hkl*
13	6	2.041	2.0486	$\bar{1}51$
	4		2.0089	$\bar{3}32$
30	7	1.956	1.9580	241
	5		1.9563	$\bar{1}34$
	15		1.9506	151
7	4	1.904	1.9058	321
13	8	1.858	1.8562	114
	5		1.8229	250
18	4	1.809	1.8116	$\bar{2}52$
	7		1.8009	$\bar{3}42$
30	3	1.784	1.7924	060
	10		1.7906	$\bar{4}11$
	9		1.7812	143
	12		1.7693	$\bar{1}53$
45	3	1.752	1.7556	061
	10		1.7520	312
	13		1.7489	$\bar{2}25$
	5		1.7450	$\bar{4}22$
	3		1.7432	340
30	15	1.729	1.7336	$\bar{3}34$
	4		1.7226	$\bar{3}05$
	4		1.7211	$\bar{3}43$
	8		1.7179	015
	3		1.6359	420
12	6	1.626	1.6242	341
6	3	1.587	1.5951	153
	4		1.5755	214
18	3	1.557	1.5655	035
	6		1.5539	$\bar{2}54$
	4		1.5512	243
17	4	1.524	1.5295	054
	4		1.5212	$\bar{4}42$
	3		1.5130	071
	4		1.5053	$\bar{2}63$
4	3	1.487	1.4832	323
14	6	1.450	1.4538	$\bar{1}72$
	3		1.4473	440

Calculated intensities are normalized so that the lines contributing to the highest observed line total 100. Only normalized $I_{calc} \geq 3$ are listed.

TABLE 3. DATA COLLECTION AND STRUCTURE REFINEMENT DETAILS FOR ADANITE

Diffractometer	Rigaku R-Axis Rapid II
X-ray radiation / power	Mo$K\alpha$ (λ = 0.71075 Å)/ 50 kV, 40 mA
Temperature	293(2) K
Structural Formula	$Pb_2(Te^{4+}O_3)(SO_4)$
Space group	$P2_1/n$
Unit cell dimensions	a = 7.3830(3) Å b = 10.7545(5) Å c = 9.3517(7) Å β = 111.500(8)°
V	690.86(7) Å^3
Z	4
Density (for above formula)	6.596 g/cm^3
Absorption coefficient	53.105 mm^{-1}
F(000)	1152
Crystal size	130 × 90 × 40 mm
θ range	3.01 to 29.97°
Index ranges	$-10 \leq h \leq 10$, $-15 \leq k \leq 15$, $-13 \leq l \leq 13$
Refls. collected / unique	19381 / 2011; R_{int} = 0.059
Reflections with $I > 2\sigma I$	1906
Completeness to q = 29.97°	100%
Refinement method	Full-matrix least-squares on F^2
Parameters / restraints	101 / 0
GoF	1.187
Final R indices [$I_o > 2\sigma I$]	R_1 = 0.0221, wR_2 = 0.0460
R indices (all data)	R_1 = 0.0241, wR_2 = 0.0467
Extinction coefficient	0.00116(10)
Largest diff. peak/hole	+2.21/–1.31 e/A^3

* $R_{int} = \Sigma|F_o^2 - F_o^2(\text{mean})|/\Sigma[F_o^2]$. GoF $= S = \{\Sigma[w(F_o^2 - F_c^2)^2]/(n-p)\}^{1/2}$. $R_1 = \Sigma||F_o| - |F_c||/\Sigma|F_o|$. $wR_2 = \{\Sigma[w(F_o^2 - F_c^2)^2]/\Sigma[w(F_o^2)^2]\}^{1/2}$; $w = 1/[\sigma^2 F_o^2) + (aP)^2 + bP]$ where a is 0.112, b is 3.6821 and P is $[2F_c^2 + \text{Max}(F_o^2,0)]/3$.

Renishaw inVia Qontor Raman microscope with a 3000 gr/mm diffraction grating and a low wavenumber filter. A 2 μm diameter spot from a 514.5 nm solid-state laser was focused onto the sample through a 50× objective lens using an integrated Leica microscope. The shift scale was calibrated using the 520.5 cm^{-1} Si line. The spectra of adanite recorded in the range from 2000 to 20 cm^{-1} showed very pronounced changes in relative peak intensities from grain to grain, undoubtedly reflecting strong orientation dependencies; however, features at 1098, 968, 734, ~607, 448, ~410, ~84, and ~44 cm^{-1} were present for all orientations. No degradation of the grains was observed during recording of the spectra. Representative spectra from 1200 to 20 cm^{-1} are shown in Figure 2.

While the complexity of the Raman spectrum makes a comprehensive assignment of bands impossible, the bands observed between 1200 and 300 cm^{-1} are all likely related to various stretching and bending modes of $(TeO_3)^{2-}$ and $(SO_4)^{2-}$. In particular, the band at 734 cm^{-1} is consistent with the $(TeO_3)^{2-}$ symmetric stretching mode. The band at 968 cm^{-1} and the weak but distinct band at 1098 cm^{-1} are in the range typical for minerals containing $(SO_4)^{2-}$ groups.

CHEMICAL COMPOSITION

Nine chemical analyses were obtained from two crystal fragments using a JEOL 8200 electron microprobe in WDS mode (15 kV, 5 nA, 5 μm beam diameter). No other elements were detected by EDS. The structure determination and Raman spectrum indicate adanite to be anhydrous. Analytical data are given in Table 1.

The empirical formula based on 7 anions (O + Cl) is $Pb_{1.89}Sb^{3+}_{0.02}Te^{4+}_{0.98}S^{6+}_{1.04}Cl_{0.02}O_{6.98}$. The simplified formula is $Pb_2[(Te^{4+},Sb^{3+})O_3](SO_4)$ and the ideal formula is $Pb_2(Te^{4+}O_3)(SO_4)$, which requires PbO 65.07, TeO_2 23.26, SO_3 11.67, total 100 wt.%. The Gladstone-Dale compatibility index 1 – (K_P/K_C) for the empirical formula is –0.018, indicating superior compatibility among the average index of refraction, calculated density, and chemical composition (Mandarino 2007).

X-RAY CRYSTALLOGRAPHY

Powder X-ray studies were done using a Rigaku R-Axis Rapid II curved imaging plate microdiffractometer with monochromatized Mo$K\alpha$ radiation (λ = 0.71075 Å). A Gandolfi-like motion on the φ and ω axes was used to randomize the samples. Observed d values and intensities were derived by profile fitting using JADE 2010 software. Data are given in Table 2. Unit cell parameters refined from the powder data using JADE 2010 with whole pattern fitting are a = 7.386(5), b = 10.758(5), c = 9.365(5) Å, β = 111.476(17)°, and V = 692.5(7) Å^3.

Single-crystal data were collected using the same diffractometer and radiation noted above. More than a full sphere of structure data was recorded. The Rigaku CrystalClear software package was used to process the structure data, including the application of an empirical absorption correction using the multi-scan method with ABSCOR (Higashi 2001). The structure was solved by the charge-flipping method using SHELXT (Sheldrick 2015a). Refinement proceeded by full-matrix least-squares on F^2 using SHELXL-2016 (Sheldrick 2015b). All sites refined to full occupancy.

TABLE 4. ATOM COORDINATES AND DISPLACEMENT PARAMETERS (Å^2) FOR ADAMITE

	x/a	y/b	z/c	U_{eq}
Pb1	0.13927(3)	0.65731(2)	0.50286(2)	0.01526(7)
Pb2	0.28067(3)	0.03966(2)	0.56839(2)	0.01526(7)
Te	0.39611(5)	0.36216(3)	0.69092(4)	0.00994(8)
S1	0.2752(2)	0.38111(14)	0.29373(15)	0.0143(3)
O1	0.4873(7)	0.3896(5)	0.3502(6)	0.0337(12)
O2	0.1955(8)	0.3322(5)	0.1360(5)	0.0283(10)
O3	0.2137(7)	0.2993(5)	0.3942(5)	0.0272(10)
O4	0.1934(7)	0.5077(5)	0.2920(5)	0.0262(10)
O5	0.2644(6)	0.2162(4)	0.7089(4)	0.0155(8)
O6	0.1709(6)	0.4630(4)	0.6372(5)	0.0149(8)
O7	0.4616(6)	0.4059(4)	0.9007(4)	0.0162(8)

	U^{11}	U^{22}	U^{33}	U^{23}	U^{13}	U^{12}
Pb1	0.01816(12)	0.00963(11)	0.01757(11)	0.00169(7)	0.00606(9)	–0.00152(7)
Pb2	0.01471(12)	0.01140(12)	0.01948(11)	–0.00373(7)	0.00604(8)	–0.00151(7)
Te	0.01105(17)	0.00544(16)	0.01332(15)	–0.00104(11)	0.00443(13)	–0.00027(12)
S	0.0141(6)	0.0135(7)	0.0165(6)	0.0003(5)	0.0070(5)	–0.0021(5)
O1	0.016(2)	0.034(3)	0.051(3)	0.006(2)	0.013(2)	0.001(2)
O2	0.041(3)	0.023(3)	0.019(2)	–0.0047(17)	0.009(2)	–0.001(2)
O3	0.029(2)	0.029(3)	0.023(2)	0.0049(19)	0.0080(19)	–0.011(2)
O4	0.029(2)	0.021(2)	0.031(2)	–0.0052(19)	0.013(2)	0.001(2)
O5	0.025(2)	0.0068(19)	0.0154(17)	–0.0011(14)	0.0087(16)	–0.0049(16)
O6	0.0134(19)	0.0064(19)	0.025(2)	0.0011(15)	0.0072(16)	0.0007(14)
O7	0.0156(19)	0.014(2)	0.0153(18)	–0.0052(15)	0.0017(15)	0.0020(16)

Data collection and refinement details are given in Table 3, atom coordinates and displacement parameters in Table 4, selected bond distances in Table 5, and a bond-valence analysis in Table 6. A CIF file with observed and calculated structure factors has been deposited and is available from the Depository of Unpublished Data on the MAC website [document Adanite, CM58, 20-00010][1].

ATOMIC ARRANGEMENT

The structure of adanite is the same as that of the synthetic compound with the same formula reported by Weil & Shirkhanlou (2017). It contains two different Pb^{2+} sites and one Te^{4+} site, all of which exhibit off-center coordinations, typical of cations with lone-pair electrons. The coordination of the Te site is characterized by three short cation–oxygen bonds (<1.90 Å) on one side of the Te site, defining a Te^{4+}O$_3$ pyramid with the Te^{4+} cation as its apex. This is the most typical coordinating environment for Te^{4+} in oxysalts (Christy *et al.* 2016). The Te^{4+} cation also

TABLE 5. SELECTED BOND DISTANCES (Å) FOR ADAMITE

Pb1–O6	2.405(4)	Pb2–O5	2.337(4)	Te–O5	1.886(4)	S–O1	1.460(5)
Pb1–O6	2.536(4)	Pb2–O7	2.376(4)	Te–O6	1.892(4)	S–O2	1.471(5)
Pb1–O5	2.602(4)	Pb2–O7	2.394(4)	Te–O7	1.899(4)	S–O3	1.475(5)
Pb1–O1	2.640(5)	Pb2–O6	2.769(4)	Te–O3	2.689(5)	S–O4	1.487(5)
Pb1–O4	2.686(4)	Pb2–O2	2.984(5)	Te–O1	2.873(6)	<S–O>	1.473
Pb1–O2	2.806(5)	Pb2–O4	3.041(5)	Te–O3	2.976(5)		
Pb1–O7	3.001(4)	Pb2–O3	3.178(5)	Te–O2	3.218(5)		
Pb1–O3	3.126(5)	Pb2–O2	3.203(5)	Te–O4	3.289(5)		
Pb1–O5	3.213(4)	Pb2–O4	3.462(5)	Te–O1	3.502(5)		
<Pb1–O>	2.779	<Pb2–O>	2.860	<Te–O>	2.692		

---

[1] Supplementary Data are available from the Depository of Unpublished Data on the MAC website (http://mineralogicalassociation.ca/), document "Adanite, CM58, 20-00010".

TABLE 6. BOND-VALENCE ANALYSIS FOR ADAMITE (VALUES ARE EXPRESSED IN VALENCE UNITS)

	Pb1	Pb2	Te	S	Σ
O1	0.25		0.11, 0.02	1.58	1.96
O2	0.17	0.12, 0.07	0.05	1.54	1.95
O3	0.08	0.07	0.17, 0.08	1.52	1.92
O4	0.23	0.10, 0.04	0.04	1.48	1.89
O5	0.28, 0.07	0.50	1.20		2.05
O6	0.43, 0.32	0.19	1.18		2.12
O7	0.11	0.46, 0.44	1.16		2.17
Σ	1.94	1.99	4.01	6.12	

Bond valence parameters for Pb^{2+}–O and S^{6+}–O are from Gagné & Hawthorne (2015) and those for Te^{4+}–O are from Mills & Christy (2013).

forms six much longer bonds (2.69 to 3.50 Å) to O atoms. The Pb1 and Pb2 sites both have coordinations of nine. The atom at Pb1 forms five relatively short (<2.69 Å) bonds to O atoms on the same side of the coordination sphere and four longer (2.805 to 3.213 Å) bonds to O atoms distributed in other directions. The cation at Pb2 forms three quite short (<2.40 Å) bonds to O atoms on the same side of the coordination sphere and six longer (2.769 to 3.462 Å) bonds to O atoms distributed in other directions. The SO_4 group has a normal geometry, with S–O distances from 1.460 to 1.487 Å. Each of the O atoms of the SO_4 group forms multiple long bonds to Pb^{2+} and Te^{4+} cations, the shortest being the Pb–O4 bond at 2.686 Å.

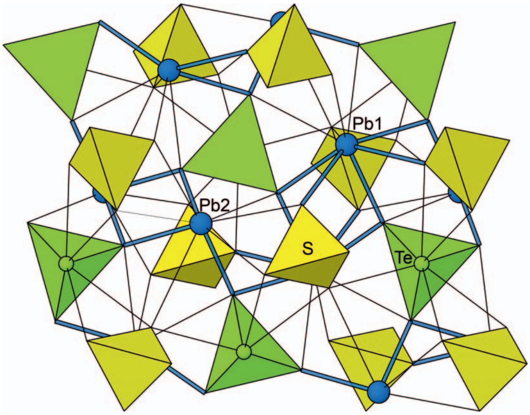

FIG. 4. One layer parallel to $10\bar{1}$ in the structure of adanite viewed down $20\bar{1}$, with [010] vertical. The SO_4 groups are shown above and below the sheets formed by linkages between Pb^{2+} cations and the O atoms of the $Te^{4+}O_3$ pyramids. The short Pb^{2+}–O bonds (<2.7 Å) are shown as blue lines. The long Pb^{2+}–O and Te^{4+}–O bonds are shown as thin black lines.

The structure (Fig. 3) exhibits relatively uniform connectivity in three dimensions, which explains the conchoidal fracture and lack of cleavage. The strongly bonded structural units, the $Te^{4+}O_3$ pyramid and SO_4 tetrahedron, do not form strong bonds with one another. The strongest bonds between structural units are the short bonds between the Pb^{2+} cations and the O atoms of the $Te^{4+}O_3$ pyramid. These linkages form

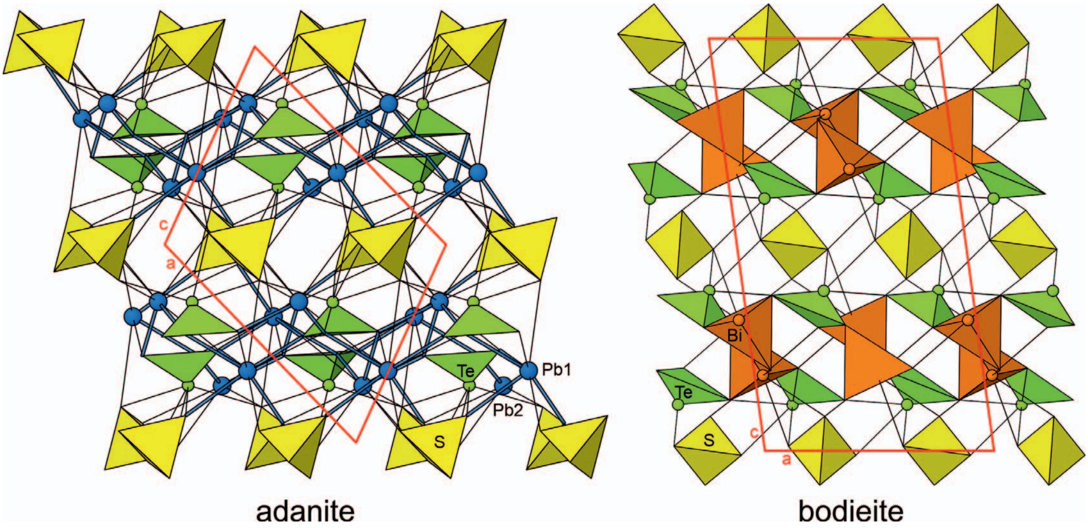

FIG. 3. The structures of adanite and bodieite along **b**. The three short Bi^{3+}–O bonds in bodieite are shown as $Bi^{3+}O_3$ pyramids. The short Pb^{2+}–O bonds (<2.7 Å) in adanite are shown as blue sticks. The long Pb^{2+}–O, Bi^{3+}–O, and Te^{4+}–O bonds in the structures are shown as thin black lines. The unit cell outlines are red.

sheets parallel to $\{10\bar{1}\}$ (Fig. 4). The relatively long bonds from the Pb^{2+} and Te^{4+} cations in the layers to the SO_4 groups between the layers link the layers to one another in the $[20\bar{1}]$ direction.

Discounting the tellurate-tellurite tlapallite, the only other mineral with essential tellurite, sulfate, and Pb^{2+} is eztlite, $Pb^{2+}{}_2Fe^{3+}{}_3(Te^{4+}O_3)_3(SO_4)O_2Cl$, which has a structure quite different from that of adanite (Missen *et al*. 2018). The recently described mineral bodieite, $Bi^{3+}{}_2(Te^{4+}O_3)_2(SO_4)$ (Kampf *et al*. 2018b), is structurally similar to adanite (Fig. 3). In the structure of bodieite, the stereoactive lone-pair cation Bi^{3+} plays much the same role as Pb^{2+} in the adanite structure by linking $Te^{4+}O_3$ pyramids into an undulating sheet. Also, similar to the adanite structure, the sheets in bodieite are linked to one another *via* long Bi^{3+} and Te^{4+} bonds to interlayer SO_4 groups.

Finally, although adanite and northstarite both have structures with connectivities dominated by strong Te^{4+}–O and Pb^{2+}–O bonds, and the minerals occur in intimate association, the structures are quite different. The structure of northstarite is a framework constructed of short Pb–O and Te–O bonds with channels containing S_2O_3 groups, which are only weakly bonded to the framework. It is noteworthy, however, that in both structures the S^{6+} oxyanion, $(S_2O_3)^2$ or $(SO_4)^{2-}$, is relatively weakly bonded to the strongly bonded Pb^{2+}–O^{2-}–Te^{4+} network.

ACKNOWLEDGMENTS

Associate Editor Maria Franca Brigatti and two anonymous reviewers are thanked for their constructive comments on the manuscript. At Caltech, the microprobe analyses and Raman studies were funded by grants from the Northern California Mineralogical Society and NSF grant EAR-1322082. The rest of this study was funded by the John Jago Trelawney Endowment to the Mineral Sciences Department of the Natural History Museum of Los Angeles County.

REFERENCES

CHRISTY, A.G., MILLS, S.J., & KAMPF, A.R. (2016) A review of the structural architecture of tellurium oxycompounds. *Mineralogical Magazine* **80**, 415–545.

GAGNÉ, O.C. & HAWTHORNE, F.C. (2015) Comprehensive derivation of bond-valence parameters for ion pairs involving oxygen. *Acta Crystallographica* **B71**, 562–578.

GUNTER, M.E., BANDLI, B.R., BLOSS, F.D., EVANS, S.H., SU, S.C., & WEAVER, R. (2004) Results from a McCrone spindle stage short course, a new version of *EXCALIBR*, and how to build a spindle stage. *The Microscope* **52**, 23–39.

HIGASHI, T. (2001) *ABSCOR*. Rigaku Corporation, Tokyo, Japan.

KAMPF, A.R., HOUSLEY, R.M., & ROSSMAN, G.R. (2018a) Pararaisaite, the dimorph of raisaite, from the North Star mine, Tintic, Utah, U.S.A. *Canadian Mineralogist* **56**, 811–820.

KAMPF, A.R., HOUSLEY, R.M., & ROSSMAN, G.R. (2018b) Bodieite, $Bi^{3+}{}_2(Te^{4+}O_3)_2(SO_4)$, a new mineral from the Tintic district, Utah, and the Masonic district, California, U.S.A. *Canadian Mineralogist* **56**, 763–772.

KAMPF, A.R., HOUSLEY, R.M., & ROSSMAN, G.R. (2020) Northstarite, a new lead-tellurite-thiosulfate mineral from the North Star mine, Tintic, Utah, U.S.A. *Canadian Mineralogist* **58** (in press).

LINDGREN, W. & LOUGHLIN, G.F. (1919) Geology and Ore Deposits of the Tintic Mining District. *United States Geological Survey Professional Paper* **107**, 276 pp.

MANDARINO, J.A. (2007) The Gladstone–Dale compatibility of minerals and its use in selecting mineral species for further study. *Canadian Mineralogist* **45**, 1307–1324.

MILLS, S.J. & CHRISTY, A.G. (2013) Revised values of the bond valence parameters for Te^{IV}–O, Te^{VI}–O and Te^{IV}–Cl. *Acta Crystallographica* **B69**, 145–149.

MISSEN, O.P., MILLS, S.J., SPRATT, J., WELCH, M.D., BIRCH, W.D., RUMSEY, M.S., & VYLITA, J. (2018) The crystal-structure determination and redefinition of eztlite, $Pb^{2+}{}_2Fe^{3+}{}_3(Te^{4+}O_3)_3(SO_4)O_2Cl$. *Mineralogical Magazine* **82**, 1355–1367.

MISSEN, O.P., RAM, R., MILLS, S.J., ETSCHMANN, B., REITH, F., SHUSTER, J., SMITH, D.J., & BRUGGER, J. (2020) Love is in the Earth: A review of tellurium (bio)geochemistry in surface environments. *Earth-Science Reviews*, 103150.

SHELDRICK, G.M. (2015a) *SHELXT* - Integrated space-group and crystal-structure determination. *Acta Crystallographica* **A71**, 3–8.

SHELDRICK, G.M. (2015b) Crystal Structure refinement with *SHELX*. *Acta Crystallographica* **C71**, 3–8.

WEIL, M. & SHIRKHANLOU, M. (2017) Incorporation of sulfate or selenate groups into oxotellurates (IV): II. Compounds with divalent lead. *Zeitschrift für anorganische und allgemeine Chemie* **643**, 757–765.

Received February 7, 2020. Revised manuscript accepted March 25, 2020.